Bilayer Heisenberg model studied by the Schwinger-boson Gutzwiller-projection method

T. Miyazaki, I. Nakamura, and D. Yoshioka
Institute of Physics, College of Arts and Sciences, University of Tokyo Komaba, Meguro-ku, Tokyo 153, Japan
(Received 13 November 1995)

A two-dimensional, bilayer, square lattice Heisenberg model with different intraplane ($J_\parallel$) and interplane ($J_\perp$) couplings is investigated. The model is first solved in the Schwinger-boson mean-field approximation. Then the solution is Gutzwiller projected to satisfy the local constraint that there should be only one boson at each site. For these wave functions, we perform variational Monte Carlo simulation up to $24\times24\times2$ sites. It is shown that the Néel order is destroyed as the interplane coupling is increased. The obtained critical value, $J_\perp/J_\parallel=3.51$, is smaller than that obtained by the mean-field theory. The excitation spectrum is calculated by a single-mode approximation. It is shown that the energy gap develops once the Néel order is destroyed.

I. INTRODUCTION

The spin pseudogap observed in underdoped $YBa_2Cu_3O_{7-x}$ is one of the fascinating characteristics of the high-T_c cuprates. NMR experiments showed that even above the transition temperature of superconductivity, T_c, the static uniform susceptibility and the NMR relaxation rate T_1 decrease with decreasing temperature.[1] Neutron scattering experiments showed the decrease of low-energy magnetic excitation with decreasing temperature and found the precursor of a finite spin gap.[2] It has been pointed out that these astonishing experimental results can be explained provided that there is a spin pseudogap in the normal state of high-T_c materials. These phenomena indicating the spin pseudogap, however, have not been observed in the $La_{2-x}Sr_xCuO_4$ systems.[3] Therefore it is speculated that the number of CuO_2 layers between the insulating layers is essential for the formation of this gap, although a successful theory has not been presented.[4–11]

It is conceivable that the finite concentration of holes affects the spin configuration and the excitation considerably. However, as a first step toward understanding of the spin pseudogap behavior, it is meaningful to study the properties of the bilayer CuO_2 system at zero doping; namely, we investigate a bilayer square lattice Heisenberg model of spin 1/2:

$$H=J_\parallel\sum_i\sum_w\sum_{a=1,2}\boldsymbol{S}_{i,a}\cdot\boldsymbol{S}_{i+w,a}+J_\perp\sum_i\boldsymbol{S}_{i,1}\cdot\boldsymbol{S}_{i,2}, \quad (1)$$

where $w=x,y$, $i+w$ represents a site next to the site i in the w direction, and $\boldsymbol{S}_{i,a}$ is a spin 1/2 operator at site i in plane a. The nearest neighbor spins interact antiferromagnetically with the intraplane coupling constant $J_\parallel$ and interplane coupling constant $J_\perp$. What we want to know is how the properties of the system change as $J_\perp/J_\parallel\equiv\alpha$ increases: at what value of α is the Néel order destroyed, and how the excitation spectrum varies.

As for the zero-temperature critical value of α_c for the destruction of the Néel order, there have been several investigations by various methods: the spin wave approximation given by Matsuda and Hida[12,13] and the Schwinger-boson mean-field theory[7,8] resulted in a quite large critical value, $\alpha_c=4.24$ for the former and 4.48 for the latter. On the other hand, more sophisticated methods have resulted in much lower critical values. Quantum Monte Carlo calculation gives it as 2.51 ± 0.01,[14] and the dimer expansion, which is an approach from the $\alpha\to\infty$ limit, gives 2.56.[15] One of the aims of the present paper is to obtain this critical value by another method, the Schwinger-boson Gutzwiller-projection method.

In the Schwinger-boson Gutzwiller-projection method we first solve the Hamiltonian by the Schwinger-boson mean-field theory.[16,17] The obtained ground-state wave function is Gutzwiller projected to fix the spin at each site to be 1/2. The wave function thus obtained is a kind of resonating valence bond[18,19] (RVB) wave function where long-range bonds are allowed with amplitude depending on the distance between the sites.[20] This method was first used by Chen and Xiu for the square lattice antiferromagnetic Heisenberg model.[21] It was shown that the wave function obtained this way is quite close to the true ground state. This method has also been applied to the anisotropic Heisenberg model.[22] There it was shown that even in the one-dimensional limit the ground-state energy, $-0.4377J$ per site, is quite close to the exact value, $-0.4431J$ per site.[23] Therefore we expect that this method gives wave functions quite close to the actual ground state in the present system, too. A merit of the present method is that the wave function is given as a RVB wave function. Thus the vertically coupled dimer state in the limit of $\alpha\to\infty$, the disordered state at intermediate values of α, and the Néel state at small α can be described in a unified way by wave functions with the same structure.

In this paper, using this method we show that the Néel order at small α is destroyed at $\alpha_c=3.51$. It is expected that a gap appears in the excitation spectrum at $\alpha>\alpha_c$. This is confirmed by our calculation of the spectrum by a single-mode approximation. To obtain these results we solve the present Hamiltonian by the Schwinger-boson mean-field theory in Sec. II. The obtained ground-state wave function is Gutzwiller projected in Sec. III. The single mode approximation for the RVB wave function is discussed in Sec. IV. In

Sec. V, we perform a variational Monte Carlo simulation for these wave functions and calculate its energy, spin-spin correlation, staggered magnetization, and low-lying excitation spectrum. In Sec. VI the critical point and the excitation spectrum are discussed.

II. MEAN-FIELD SOLUTION

We introduce four kinds of Bose operators, $s_{i,a,\uparrow}$ and $s_{i,a,\downarrow}$ $(a=1,2)$, to express the spin operators

$$S^{+}_{i,a}=s^{\dagger}_{i,a,\uparrow}s_{i,a,\downarrow}, \quad S^{z}_{i,a}=\frac{1}{2}(s^{\dagger}_{i,a,\uparrow}s_{i,a,\uparrow}-s^{\dagger}_{i,a,\downarrow}s_{i,a,\downarrow}). \tag{2}$$

The commutation relations of the spin operators $\boldsymbol{S}_i$ are satisfied in this replacement. We impose a constraint,

$$s^{\dagger}_{i,a,\uparrow}s_{i,a,\uparrow}+s^{\dagger}_{i,a,\downarrow}s_{i,a,\downarrow}=1, \tag{3}$$

in order to guarantee $S=1/2$. Then the Hamiltonian is rewritten as

$$\begin{aligned}H=&\frac{1}{2}J_{\parallel}\sum_{i}\sum_{w}\sum_{a=1,2}\sum_{\sigma}(s^{\dagger}_{i,a,\sigma}s^{\dagger}_{i+w,a,-\sigma}s_{i+w,a,\sigma}s_{i,a,-\sigma}\\&-s^{\dagger}_{i,a,\sigma}s^{\dagger}_{i+w,a,-\sigma}s_{i+w,a,-\sigma}s_{i,a,\sigma})\\&+\frac{1}{2}J_{\perp}\sum_{i}\sum_{\sigma}(s^{\dagger}_{i,1,\sigma}s^{\dagger}_{i,2,-\sigma}s_{i,2,\sigma}s_{i,1,-\sigma}\\&-s^{\dagger}_{i,1,\sigma}s^{\dagger}_{i,2,-\sigma}s_{i,2,-\sigma}s_{i,1,\sigma})+\mu\sum_{i}\sum_{a=1,2}\sum_{\sigma}s^{\dagger}_{i,a,\sigma}s_{i,a,\sigma}.\end{aligned} \tag{4}$$

Here μ is a chemical potential introduced to enforce the constraint Eq. (3) on the average. To solve the Hamiltonian in the mean-field approximation, we introduce the mean-field order parameters $\Delta_{w,a}$, Δ_z, and $n_{a,\sigma}$, which give the amplitudes of the intralayer singlet correlations, interlayer singlet correlations, and an averaged occupation number, respectively:

$$\Delta_w\equiv\Delta_{w,2}=-\Delta_{w,1}=\frac{1}{2}\langle s_{i,2,\downarrow}s_{i+w,2,\uparrow}-s_{i,2,\uparrow}s_{i+w,2,\downarrow}\rangle, \tag{5}$$

$$\Delta_z=\frac{1}{2}\langle s_{i,1,\downarrow}s_{i,2,\uparrow}-s_{i,1,\uparrow}s_{i,2,\downarrow}\rangle, \tag{6}$$

$$n_{a,\sigma}=\langle s^{\dagger}_{i,a,\sigma}s_{i,a,\sigma}\rangle=\frac{1}{2}. \tag{7}$$

After decoupling the Hamiltonian, we rewrite the operator using its Fourier transformation:

$$s_{i,a,\sigma}=\frac{1}{\sqrt{N}}\sum_{k}e^{i\boldsymbol{k}\cdot\boldsymbol{r}_i}s_{k,a,\sigma}, \tag{8}$$

where N is the total number of lattice sites for each layer, and $\boldsymbol{k}$ summation is taken over the Brillouin zone $-\pi\leqslant k_x\leqslant\pi$, $-\pi\leqslant k_y\leqslant\pi$. The mean-field Hamiltonian H_{MF} is written as

$$\begin{aligned}H_{\mathrm{MF}}=&\sum_{k}\sum_{a}\lambda(s^{\dagger}_{k,a,\uparrow}s_{k,a,\uparrow}+s^{\dagger}_{-k,a,\downarrow}s_{-k,a,\downarrow})\\&+i\gamma_k(s^{\dagger}_{k,2,\uparrow}s^{\dagger}_{-k,2,\downarrow}-s^{\dagger}_{k,1,\uparrow}s^{\dagger}_{-k,1,\downarrow})-i\gamma^{\star}_k(s_{k,2,\uparrow}s_{-k,2,\downarrow}\\&-s_{k,1,\uparrow}s_{-k,1,\downarrow})-i\delta^{\star}(s_{k,1,\uparrow}s_{-k,2,\downarrow}-s_{k,2,\uparrow}s_{-k,1,\downarrow})\\&+i\delta(s^{\dagger}_{k,1,\uparrow}s^{\dagger}_{-k,2,\downarrow}-s^{\dagger}_{k,2,\uparrow}s^{\dagger}_{-k,1,\downarrow})+\mathrm{const}\end{aligned} \tag{9}$$

with

$$\lambda=\mu-J_{\parallel}, \tag{10}$$

$$\gamma_k=2J_{\parallel}(\Delta_x\sin k_x+\Delta_y\sin k_y), \tag{11}$$

$$\delta=-iJ_{\perp}\Delta_z. \tag{12}$$

The Hamiltonian can be diagonalized by a paraunitary Bogoliubov transformation,

$$\begin{aligned}s_{k,1,\uparrow}=&\frac{1}{\sqrt{2}}(\cosh\theta^{+}_k\alpha_{k\uparrow}-\cosh\theta^{-}_k\beta_{k\uparrow}+i\sinh\theta^{+}_k\alpha^{\dagger}_{-k\downarrow}\\&-i\sinh\theta^{-}_k\beta^{\dagger}_{-k\downarrow}),\end{aligned} \tag{13}$$

$$\begin{aligned}s^{\dagger}_{-k,1,\downarrow}=&\frac{1}{\sqrt{2}}(i\sinh\theta^{+}_k\alpha_{k\uparrow}-i\sinh\theta^{-}_k\beta_{k\uparrow}-\cosh\theta^{+}_k\alpha^{\dagger}_{-k\downarrow}\\&+\cosh\theta^{-}_k\beta^{\dagger}_{-k\downarrow}),\end{aligned} \tag{14}$$

$$\begin{aligned}s_{k,2,\uparrow}=&\frac{1}{\sqrt{2}}(\cosh\theta^{+}_k\alpha_{k\uparrow}+\cosh\theta^{-}_k\beta_{k\uparrow}+i\sinh\theta^{+}_k\alpha^{\dagger}_{-k\downarrow}\\&+i\sinh\theta^{-}_k\beta^{\dagger}_{-k\downarrow}),\end{aligned} \tag{15}$$

$$\begin{aligned}s^{\dagger}_{-k,2,\downarrow}=&\frac{1}{\sqrt{2}}(-i\sinh\theta^{+}_k\alpha_{k\uparrow}-i\sinh\theta^{-}_k\beta_{k\uparrow}+\cosh\theta^{+}_k\alpha^{\dagger}_{-k\downarrow}\\&+\cosh\theta^{-}_k\beta^{\dagger}_{-k\downarrow}),\end{aligned} \tag{16}$$

where

$$\begin{aligned}\cosh\theta^{\pm}_k&=\sqrt{\frac{\lambda+E_{k\pm}}{2E_{k\pm}}},\\\sinh\theta^{\pm}_k&=-\sqrt{\frac{\lambda-E_{k\pm}}{2E_{k\pm}}}\,\mathrm{sgn}(\gamma_k\pm\delta),\end{aligned} \tag{17}$$

$$E_{k\pm}=\sqrt{\lambda^2-(\gamma_k\pm\delta)^2}. \tag{18}$$

After the transformation, the Hamiltonian finally becomes

$$\begin{aligned}H_{\mathrm{MF}}=&\sum_{k}E_{k+}(\alpha^{\dagger}_{k\uparrow}\alpha_{k\uparrow}+\alpha^{\dagger}_{-k\downarrow}\alpha_{-k\downarrow})\\&+E_{k-}(\beta^{\dagger}_{k\uparrow}\beta_{k\uparrow}+\beta^{\dagger}_{-k\downarrow}\beta_{-k\downarrow})+\mathrm{const.}\end{aligned} \tag{19}$$

The ground state $|G\rangle$ is defined as the vacuum of the Bose operator $\alpha_{k\uparrow}$, $\alpha_{-k\downarrow}$, $\beta_{k\uparrow}$, and $\beta_{-k\downarrow}$, such that $\alpha_{k\uparrow}|G\rangle=\alpha_{-k\downarrow}|G\rangle=\beta_{k\uparrow}|G\rangle=\beta_{-k\downarrow}|G\rangle=0$.

For a finite-size system, the self-consistent equations for λ, Δ_x, Δ_y, and Δ_z are given by Eqs. (5)–(7), which lead to

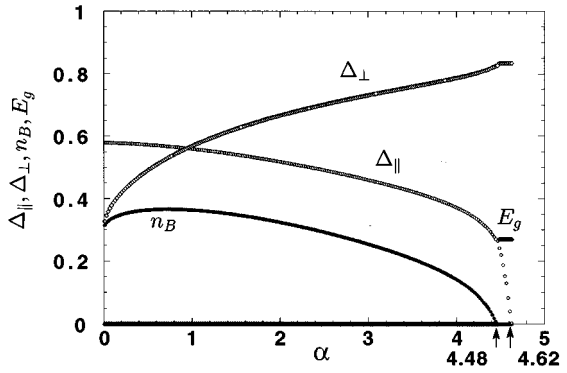

FIG. 1. Mean-field values of order parameters $\Delta_{\|}$ and $\Delta_{\perp}$, Bose condensate n_B, and energy gap E_g as a function of α.

$$1=\frac{1}{4N}\sum_k \left(\frac{\lambda}{E_{k+}}+\frac{\lambda}{E_{k-}}\right), \tag{20}$$

$$\Delta_w=\frac{1}{4N}\sum_k \sin k_w\left(\frac{\gamma_k+\delta}{E_{k+}}+\frac{\gamma_k-\delta}{E_{k-}}\right), \tag{21}$$

$$\Delta_z=\frac{i}{4N}\sum_k \left(\frac{\gamma_k+\delta}{E_{k+}}-\frac{\gamma_k-\delta}{E_{k-}}\right). \tag{22}$$

We find that the free energy takes the same minimal value for $\Delta_x=\Delta_y$ (s wave) and $\Delta_x=-\Delta_y$ (d wave).[24,25] Since either state gives the same result, we consider only the s-wave state from now on. We denote $\Delta_x=\Delta_y\equiv\Delta_{\|}$ and $-i\Delta_z\equiv\Delta_{\perp}$. The solution depends on the size of the system, N. When N is finite, $E_{k\pm}$ never becomes zero. However, in the limit of $N\to\infty$ it is possible that $E_{k\pm}$ vanishes at $\boldsymbol{k}=\boldsymbol{K}_{\pm}=\pm(\pi/2,\pi/2)$. In such a case it is known that we need to introduce the Bose condensate n_B, and Eqs. (20)–(22) are rewritten as

$$1=\frac{1}{4(2\pi)^2}\int_{-\pi}^{\pi}\int_{-\pi}^{\pi}\left(\frac{\lambda}{E_{k+}}+\frac{\lambda}{E_{k-}}\right)dk_x dk_y+n_B, \tag{23}$$

$$\Delta_{\|}=\frac{1}{4(2\pi)^2}\int_{-\pi}^{\pi}\int_{-\pi}^{\pi}\sin k_w\left(\frac{\gamma_k+\delta}{E_{k+}}+\frac{\gamma_k-\delta}{E_{k-}}\right)dk_x dk_y+n_B, \tag{24}$$

$$\Delta_{\perp}=\frac{1}{4(2\pi)^2}\int_{-\pi}^{\pi}\int_{-\pi}^{\pi}\left(\frac{\gamma_k+\delta}{E_{k+}}-\frac{\gamma_k-\delta}{E_{k-}}\right)dk_x dk_y+n_B. \tag{25}$$

When the Bose condensate n_B becomes finite, we have $\lambda=4J_{\|}\Delta_{\|}+J_{\perp}\Delta_{\perp}$. The self-consistent equations are numerically solved. Figure 1 shows the α dependence of order parameters $\Delta_{\|}$ and $\Delta_{\perp}$, Bose condensate n_B, and energy gap E_g. The Bose condensate vanishes at $\alpha=4.48$, and the gap opens for $\alpha>4.48$. The intralayer RVB order parameter $\Delta_{\|}$ vanishes at $\alpha=4.62$. For $\alpha>4.62$, only the interlayer nearest neighbor spin-spin correlation exists.

The intra- (inter-) layer spin-spin correlation $\langle \boldsymbol{S}_{i,a}\cdot\boldsymbol{S}_{j,a}\rangle$ ($\langle \boldsymbol{S}_{i,1}\cdot\boldsymbol{S}_{j,2}\rangle$) in the ground state is given as

$$\langle \boldsymbol{S}_{i,a}\cdot\boldsymbol{S}_{j,a}\rangle=\frac{3}{2}\left[\frac{1}{4N}\sum_k\left(\frac{\lambda}{E_{k+}}+\frac{\lambda}{E_{k-}}\right)\cos\boldsymbol{k}\cdot\boldsymbol{r}_{i,j}+n_B\cos\boldsymbol{K}_+\cdot\boldsymbol{r}_{i,j}\right]^2-\frac{3}{2}\left[\frac{1}{4N}\sum_k\left(\frac{\gamma_k+\delta}{E_{k+}}+\frac{\gamma_k-\delta}{E_{k-}}\right)\sin\boldsymbol{k}\cdot\boldsymbol{r}_{i,j}+n_B\sin\boldsymbol{K}_+\cdot\boldsymbol{r}_{i,j}\right]^2, \tag{26}$$

$$\langle \boldsymbol{S}_{i,1}\cdot\boldsymbol{S}_{j,2}\rangle=\frac{3}{2}\left[\frac{1}{4N}\sum_k\left(\frac{\lambda}{E_{k+}}-\frac{\lambda}{E_{k-}}\right)\sin\boldsymbol{k}\cdot\boldsymbol{r}_{i,j}+n_B\sin\boldsymbol{K}_+\cdot\boldsymbol{r}_{i,j}\right]^2-\frac{3}{2}\left[\frac{1}{4N}\sum_k\left(\frac{\gamma_k+\delta}{E_{k+}}-\frac{\gamma_k-\delta}{E_{k-}}\right)\times\cos\boldsymbol{k}\cdot\boldsymbol{r}_{i,j}+n_B\cos\boldsymbol{K}_+\cdot\boldsymbol{r}_{i,j}\right]^2, \tag{27}$$

where $\boldsymbol{r}_{i,j}=\boldsymbol{r}_i-\boldsymbol{r}_j$. The summations over k in Eqs. (26) and (27) vanish in the limit $|r_{i,j}|\to\infty$. Therefore the correlation extends to infinity only if $n_B>0$, which means the existence of antiferromagnetic long-range order. Thus, in the mean-field approximation, the critical point of the order-disorder transition is 4.48.

III. RVB WAVE FUNCTION

The ground-state wave function obtained in the mean-field theory is expressed as

$$|G\rangle=\prod_k \exp\left[i\frac{\tanh\theta_k^+ +\tanh\theta_k^-}{2}(s^\dagger_{k,2,\uparrow}s^\dagger_{-k,2,\downarrow}-s^\dagger_{k,1,\uparrow}s^\dagger_{-k,1,\downarrow})-i\frac{\tanh\theta_k^+ -\tanh\theta_k^-}{2}(s^\dagger_{-k,1,\downarrow}s^\dagger_{k,2,\uparrow}-s^\dagger_{k,1,\uparrow}s^\dagger_{-k,2,\downarrow})\right]|0\rangle, \tag{28}$$

where $|0\rangle$ is the vacuum of the Schwinger bosons. By the Fourier transformation for $s^\dagger_{k,1,\uparrow}$, $s^\dagger_{-k,1,\downarrow}$, $s^\dagger_{k,2,\uparrow}$, and $s^\dagger_{-k,2,\downarrow}$, we can get a real-space representation for this ground state,

$$|G\rangle=\exp\left[\sum_{i,j} a_{i,j}(s^\dagger_{i,2,\uparrow}s^\dagger_{j,2,\downarrow}-s^\dagger_{i,1,\uparrow}s^\dagger_{j,1,\downarrow})+b_{i,j}(s^\dagger_{j,1,\downarrow}s^\dagger_{i,2,\uparrow}-s^\dagger_{i,1,\uparrow}s^\dagger_{j,2,\downarrow})\right]|0\rangle, \tag{29}$$

$$a_{i,j}=\frac{i}{2N}\sum_k [\tanh\theta_k^+ +\tanh\theta_k^-]\exp(i\boldsymbol{k}\cdot\boldsymbol{r}_{i,j}), \tag{30}$$

$$b_{i,j}=\frac{-i}{2N}\sum_k [\tanh\theta_k^+ -\tanh\theta_k^-]\exp(i\boldsymbol{k}\cdot\boldsymbol{r}_{i,j}). \tag{31}$$

It is evident that the local constraint Eq. (3) is not satisfied in this wave function. We remove this difficulty by projecting the wave function to a space where each site is singly occupied; namely, we perform the Gutzwiller projection, using the Gutzwiller projection operator P,

$$|G\rangle = P\Bigg[\sum_{i\neq j} a_{i,j}(s^{\dagger}_{i,2,\uparrow}s^{\dagger}_{j,2,\downarrow} - s^{\dagger}_{i,1,\uparrow}s^{\dagger}_{j,1,\downarrow}) + b_{i,j}(s^{\dagger}_{j,1,\downarrow}s^{\dagger}_{i,2,\uparrow} - s^{\dagger}_{i,1,\uparrow}s^{\dagger}_{j,2,\downarrow})\Bigg]^{N}|0\rangle. \tag{32}$$

From Eq. (32) it is clear that the ground state $|G\rangle$ is a RVB state. The weights of the bond, $a_{i,j}$ and $b_{i,j}$, decay proportionally to $r_{i,j}^{-3}$ except for $b_{i,j}$ at small $J_{\perp}$. Although it would be possible to regard every $a_{i,j}$ and $b_{i,j}$ as variational parameters, we here restrict them to be those given in Eqs. (30) and (31). In the case of $\alpha=0$, this restriction is justified by the result itself: Chen and Xiu[21] have shown that this choice of $a_{i,j}$ gives excellent results for the ground-state energy and the staggered magnetization. The weights $a_{i,j}$ and $b_{i,j}$ depend on $\alpha=J_{\perp}/J_{\parallel}$ through the order parameters. We consider this α in $a_{i,j}$ and $b_{i,j}$ as a variational parameter. In order to avoid confusion, we use a symbol α_p to mean the value of α used to obtain the ground state.

IV. EXCITATION SPECTRUM

Once the approximate ground state is obtained, the excitation spectrum can be calculated by a method given by Feynman for liquid ^{4}He, namely, the single-mode approximation.[26,27] The essential point of this method is to consider a low-lying excited state intuitively and calculate the excitation spectrum from a known ground state. In our case, the low-lying state of this Hamiltonian should be the spin wave excitation. Thus we consider the following excited states:

$$|E_{\pm}\rangle = (S^{-}_{k,1} \pm S^{-}_{k,2})|G\rangle, \tag{33}$$

$$S^{-}_{k,a} \equiv \frac{1}{\sqrt{N}}\sum_{i} S^{-}_{i,a}e^{i\mathbf{k}\cdot\mathbf{r}_i}, \tag{34}$$

where $|E_{\pm}\rangle$ are the variational excited states. The excitation spectrum $\omega_{\pm}(\mathbf{k})$ is calculated as

$$\omega_{\pm}(\mathbf{k}) = \frac{f_{\pm}(\mathbf{k})}{S_{\pm}(\mathbf{k})}, \tag{35}$$

$$S_{\pm}(\mathbf{k}) = \frac{1}{N}\sum_{i,j}\langle G|(S^{+}_{i,1}\pm S^{+}_{i,2})(S^{-}_{j,1}\pm S^{-}_{j,2})|G\rangle e^{i\mathbf{k}\cdot\mathbf{r}_{i,j}}, \tag{36}$$

$$\begin{aligned} f_{\pm}(\mathbf{k}) &= \frac{1}{N}\sum_{i,j}\langle G|(S^{+}_{i,1}\pm S^{+}_{i,2})[H,(S^{-}_{j,1}\pm S^{-}_{j,2})]|G\rangle e^{i\mathbf{k}\cdot\mathbf{r}_{i,j}} \\ &= \frac{J_{\parallel}}{N}\sum_{i,l,\omega'}\langle G|(S^{+}_{l,1}\pm S^{+}_{l,2})(-S^{-}_{i,1}S^{z}_{i+\omega',1}\mp S^{-}_{i,2}S^{z}_{i+\omega',2} \\ &\quad + S^{z}_{i,1}S^{-}_{i+\omega',1}\pm S^{z}_{i,2}S^{-}_{i+\omega',2})|G\rangle e^{i\mathbf{k}\cdot\mathbf{r}_{i,l}} \\ &\quad + (1\mp 1)\frac{J_{\perp}}{N}\sum_{i,l}\langle G|(S^{+}_{l,1}\pm S^{+}_{l,2})(S^{z}_{i,1}S^{-}_{i,2} \\ &\quad - S^{-}_{i,1}S^{z}_{i,2})|G\rangle e^{i\mathbf{k}\cdot\mathbf{r}_{i,l}}. \end{aligned} \tag{37}$$

Here, $\omega'=\pm x,\ \pm y,\ i+\omega'$ represents a site next to the site i in the ω' direction, $S_{\pm}(\mathbf{k})$ is the static structure factor and $f_{\pm}(\mathbf{k})$ is a three-point correlation function of spin operators. The two modes represent in-phase, $\omega_{+}(\mathbf{k})$, and out-of-phase, $\omega_{-}(\mathbf{k})$, spin excitations of the two layers.

Since $|G\rangle$ is a RVB state, we must consider a loop-covering associated with two valence bond configurations, $|c_1\rangle$ and $|c_2\rangle$, to calculate Eqs. (36) and (37).[20] For Eq. (36) we use known results,

$$\frac{\langle c_1|S^{+}_{i,a}S^{-}_{j,b}|c_2\rangle}{\langle c_1|c_2\rangle} = \begin{cases} \frac{1}{2}, & (i,a),(j,b) \text{ belong to the same loop and the same sublattice} \\ -\frac{1}{2}, & (i,a),(j,b) \text{ belong to the same loop and different sublattices} \\ 0, & (i,a),(j,b) \text{ belong to different loops.} \end{cases} \tag{38}$$

For Eq. (37) the following rule is found:

$$\frac{\langle c_1|S^{+}_{l,a}S^{-}_{i,b}S^{z}_{i+\delta,c}|c_2\rangle}{\langle c_1|c_2\rangle} = \begin{cases} \frac{1}{4}, & (i,b),(i+\delta,c) \text{ belong to the same loop and } (l,a)=(i+\delta,c) \\ -\frac{1}{4}, & (i,b),(i+\delta,c) \text{ belong to the same loop and } (l,a)=(i,b) \\ 0 & \text{otherwise.} \end{cases} \tag{39}$$

Here, $i+\delta$ means the nearest neighbor of the ith site. $S_{\pm}(\boldsymbol{k})$ can be calculated directly from the first rule. Using the second rule, $f_{\pm}(\boldsymbol{k})$ becomes

$$f_{\pm}(\mathbf{k})=\frac{J_{\parallel}}{N}(2-\cos k_x-\cos k_y)$$
$$\times\sum_i\sum_w\sum_{a=1,2}\langle G|S^{+}_{i+w,a}S^{-}_{i,a}S^{z}_{i+w,a}|G\rangle$$
$$+\frac{4(1\mp1)J_{\perp}}{N}\sum_i\langle G|S^{+}_{i,2}S^{-}_{i,1}S^{z}_{i,2}|G\rangle. \quad (40)$$

Thus we have only to count the number of nearest neighbors in the same loop for each loop covering. This simplifies the numerical calculation.

V. NUMERICAL RESULTS

In this section, we show numerical results of the ground-state energy, spin-spin correlation, staggered magnetization, and excitation spectrum as a function of α. We perform Monte Carlo simulations in which RVB states are sampled to satisfy detailed balance for lattices with $L\times L\times 2$ sites, where $L\leqslant 24$. All the numerical calculations are performed with periodic boundary conditions. For each system size we solve the self-consistent equations (20)–(22), and calculate $a_{i,j}$, and $b_{i,j}$ to be used to construct the wave function at that system size.

A. Ground-state energy

The energy per site of the bilayer Heisenberg model, E, is given by the nearest neighbor spin-spin correlations $\epsilon_{\parallel}(L,\alpha_p)$ and $\epsilon_{\perp}(L,\alpha_p)$ for a given wave function specified by the parameter α_p:

$$E(L,\alpha_p)=2J_{\parallel}\epsilon_{\parallel}(L,\alpha_p)+\frac{1}{2}J_{\perp}\epsilon_{\perp}(L,\alpha_p), \quad (41)$$

where

$$\epsilon_{\parallel}(L,\alpha_p)=\frac{1}{4L^2}\sum_i\sum_w\sum_{a=1,2}\langle G|\boldsymbol{S}_{i,a}\cdot\boldsymbol{S}_{i+w,a}|G\rangle, \quad (42)$$

$$\epsilon_{\perp}(L,\alpha_p)=\frac{1}{L^2}\sum_i\langle G|\boldsymbol{S}_{i,1}\cdot\boldsymbol{S}_{i,2}|G\rangle. \quad (43)$$

To estimate the energy in the thermodynamic limit, the size dependence is examined and we find the following size scaling for any fixed α_p:

$$\epsilon_{\parallel}(L,\alpha_p)=\epsilon_{\parallel}(\alpha_p)+\lambda L^{-3}+\cdots, \quad (44)$$

$$\epsilon_{\perp}(L,\alpha_p)=\epsilon_{\perp}(\alpha_p)+\lambda L^{-3}+\cdots, \quad (45)$$

where λ is a constant. This size scaling coincides with the spin wave theory for a square lattice. In Fig. 2, $\epsilon_{\parallel}(\alpha_p)$ and $\epsilon_{\perp}(\alpha_p)$ are shown. Open circles and solid circles indicate $\epsilon_{\parallel}(\alpha_p)$ and $\epsilon_{\perp}(\alpha_p)$. Error bars show the standard deviation of the Monte Carlo simulation. The interplane nearest neighbor spin-spin correlation $\epsilon_{\parallel}$ has a value of -0.3333 ± 0.0006 at $\alpha_p=0$, which is quite close to the best estimated value of -0.3348.[28,29] The magnitude of $\epsilon_{\parallel}$ decreases as α_p increases and finally vanishes at $\alpha_p=4.62$. On the other hand, the magnitude of $\epsilon_{\perp}(\alpha_p)$ increases and saturates to 0.75 at $\alpha_p=4.62$. At $\alpha_p\geqslant 4.62$ the intraplane spin correlation vanishes and the dimerized state is realized.

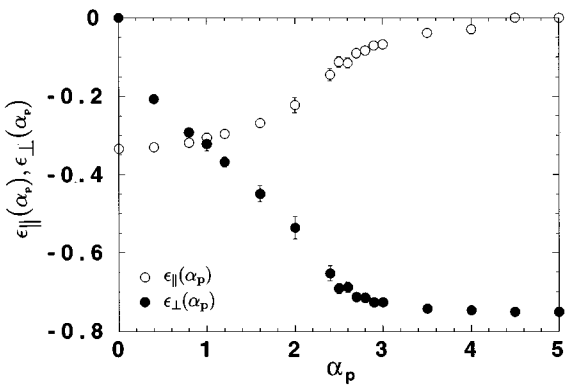

FIG. 2. The nearest neighbor spin correlation for each direction is shown. Open circles are for $\epsilon_{\parallel}$, and solid circles are for $\epsilon_{\perp}$. Error bars result from Monte Carlo statistical errors.

The ground-state energy per site at a given α is calculated as a minimum of $E(\alpha_p)=2J_{\parallel}\epsilon_{\parallel}(\alpha_p)+\frac{1}{2}J_{\perp}\epsilon_{\perp}(\alpha_p)$ with respect to α_p. Thus we can get an optimal variational parameter and energy for a given α. The relation between the variational parameter (α_p) and a real coupling (α) is shown in Fig. 3, and the ground-state energy per site is shown in Fig. 4. In Fig. 4 we also show the energy of the dimerized state per site, $-\frac{3}{8}\alpha J_{\parallel}$ (straight line), for reference. The difference between the optimal energy and the dimerized energy becomes smaller with increasing interlayer coupling.

B. Staggered magnetization

We calculated the spin-spin correlation, $\langle\boldsymbol{S}_{i,a}\cdot\boldsymbol{S}_{j,b}\rangle$, between two arbitrary sites (i,a) and (j,b). The results for a $24\times24\times2$ lattice system are shown in Fig. 5, where the absolute value of the intralayer spin-spin correlation is plotted as a function of the distance between the two sites. Open circles are for $\alpha=0.4$ and solid circles are for $\alpha=4.6$. It is obvious that there is a long-range order at $\alpha=0.4$ and no long-range order at $\alpha=4.6$. In the latter case, the correlation

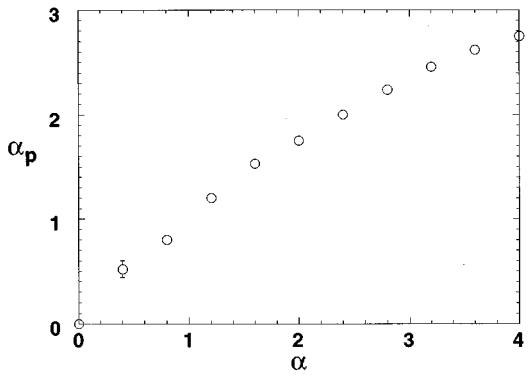

FIG. 3. The variational parameter α_p which minimizes the ground-state energy for a given parameter α.

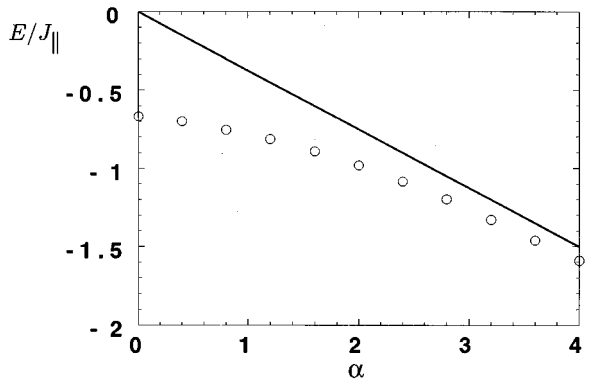

FIG. 4. Total energy per site as a function of α. Open circles are for variational Monte Carlo results and the straight line is for dimerized state, -0.375α.

decreases exponentially and the typical correlation length for the disordered state is of the order of a lattice constant.

The long-range order is of the antiferromagnetic type. In the ordered phase the staggered magnetization of the infinite-size system is obtained from the size dependence of the staggered spin-spin correlation between the most separated pairs. For a given lattice size L, we calculated both the intralayer correlation $M_0(L)^2$ and the interlayer correlation $M_1(L)^2$:

$$M_0(L)^2 \equiv \frac{1}{2N}\sum_{i,j}{}' \sum_{a=1,2} \langle |\boldsymbol{S}_{i,a}\cdot \boldsymbol{S}_{j,a}| \rangle, \tag{46}$$

$$M_1(L)^2 \equiv \frac{1}{N}\sum_{i,j}{}' \langle |\boldsymbol{S}_{i,1}\cdot \boldsymbol{S}_{j,2}| \rangle, \tag{47}$$

where the summation is taken for all the pairs of i and j such that $\boldsymbol{r}_i - \boldsymbol{r}_j = (\pm L/2, \pm L/2)$.

Except at $\alpha = 0$, $M_0(L)$ and $M_1(L)$ coincide within the Monte Carlo statistical error. As shown in Fig. 6, they are well fitted by the size scaling

$$M_0(L) = M_1(L) = M(\infty) + \mu L^{-1} + \cdots, \tag{48}$$

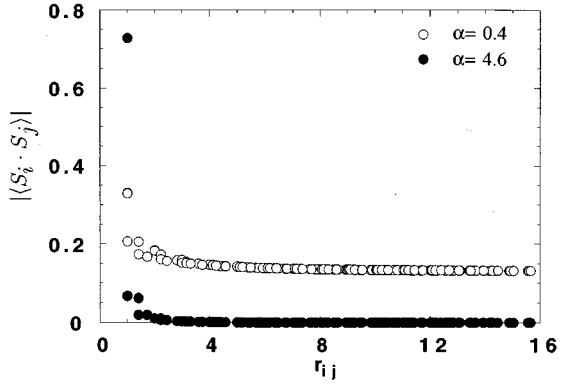

FIG. 5. Spin-spin correlation for $\alpha = 0.4$ (open circles) and $\alpha = 4.6$ (solid circles). Each calculation is done for a $24\times24\times2$ lattice. Here, $r_{i,j}$ means the distance between two sites. It is obvious that there is a long-range order for $\alpha = 0.4$ but no long-range order for $\alpha = 4.6$.

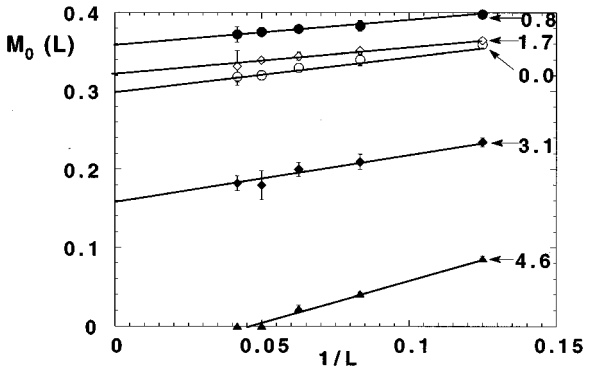

FIG. 6. $M_0(L)$ versus $1/L$ for $\alpha = 0.0$, 0.8, 1.7, 3.1, and 4.6.

where μ is a constant. This scaling agrees with the prediction of the spin wave theory and arguments given by Huse.[30] The staggered magnetization $M_0 = M(\infty)$ as a function of α is given in Fig. 7. In this figure, the results of the mean-field theory (MFT) are also shown. In the case of small α, the interlayer coupling enhances the antiferromagnetic long-range order. This is because the system acquires a weak three dimensionality and quantum fluctuation is suppressed. On the other hand, for larger α, the magnetizations are suppressed. This behavior is consistent with the result of Matsuda and Hida in the spin wave theory.[12] The staggered magnetization vanishes at $\alpha_c = 3.51 \pm 0.05$.

C. Excitation spectrum

We calculate the structure factor $S_{\pm}(\boldsymbol{k})$ and excitation spectrum $\omega_{\pm}(\boldsymbol{k})$ as a function of coupling α. The calculations are done for a $24\times24\times2$ lattice. The behavior of $S_{\pm}(\boldsymbol{k})$ and $\omega_{\pm}(\boldsymbol{k})$ strongly depends on whether the system has long-range order or not. The result for $S_{\pm}(\boldsymbol{k})$ is shown in Fig. 8 and $\omega_{\pm}(\boldsymbol{k})$ is shown in Fig. 9. Here, three typical couplings are taken: $\alpha = 0.4$ (open circles), $\alpha = 2.4$ (closed circles), and $\alpha = 3.6$ (open squares). The third coupling is for the system in the disordered phase. For each figure, (a) is for

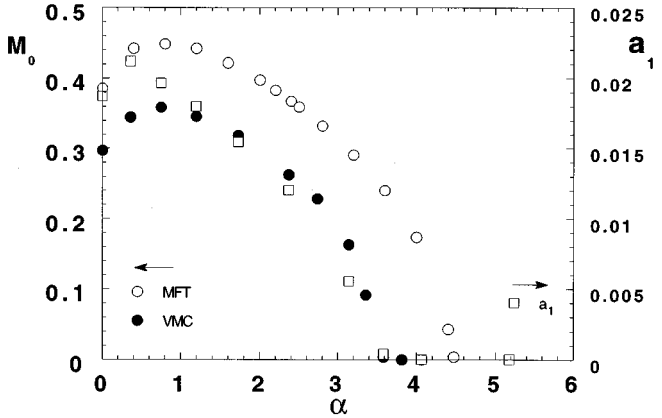

FIG. 7. Staggered magnetization as a function of α. Open circles are for the mean-field theory and solid circles are for variational Monte Carlo results. The magnitude of the k-linear term in the expansion of $S_+(\boldsymbol{k})$ around the Γ point, a_1, is also shown by open squares.

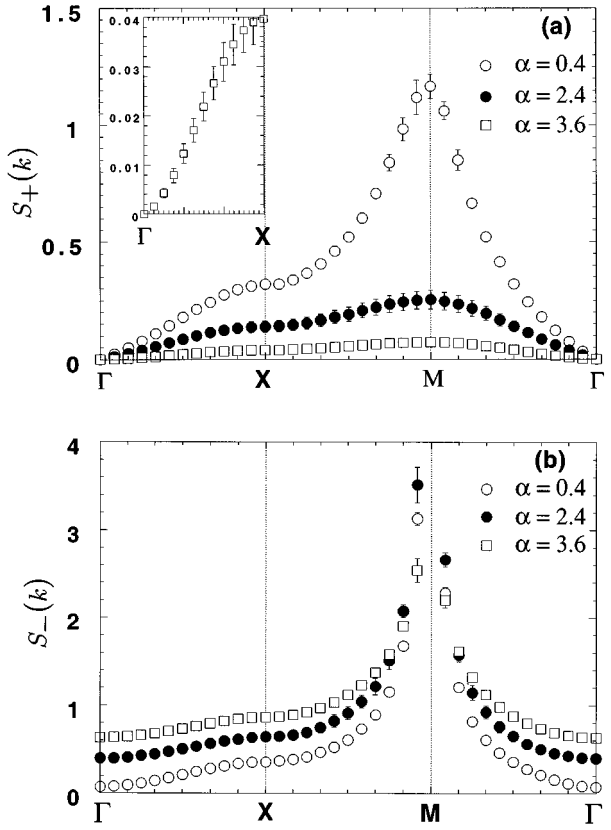

FIG. 8. The structure factors (a) $S_+(\boldsymbol{k})$ and (b) $S_-(\boldsymbol{k})$. Open circles, closed circles, and open squares are for $\alpha=0.4$, 2.4, and 3.6, respectively. Inset shows the detailed structure of $\alpha=3.6$ along the Γ-X line. Note that the value at the M point of $S_-(\boldsymbol{k})$ is too large to be shown in the figure.

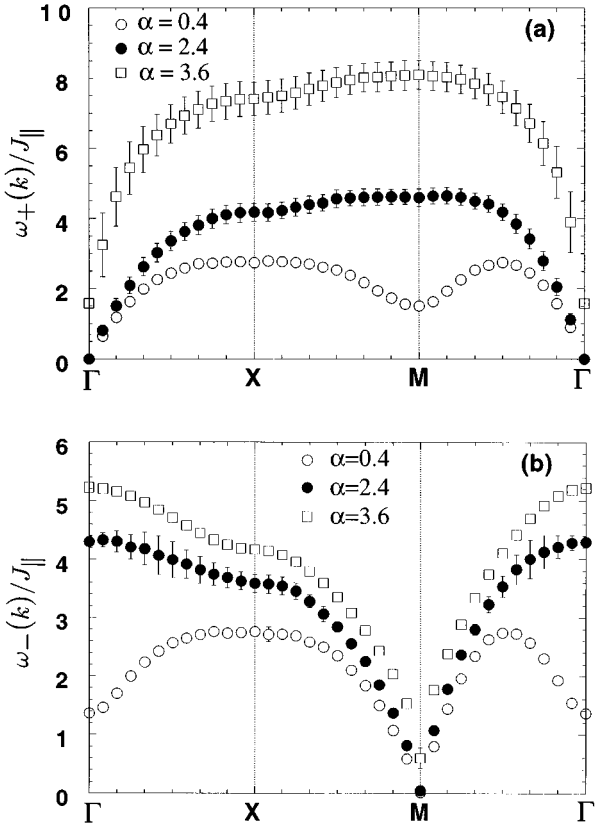

FIG. 9. Excitation spectrum (a) $\omega_+(\boldsymbol{k})$ and (b) $\omega_-(\boldsymbol{k})$. The same values for α are chosen and indicated by the same symbols as in Fig. 8. At $\alpha=3.6$, a gap opens at the Γ point for $\omega_+(\boldsymbol{k})$ and at the M point for $\omega_-(\boldsymbol{k})$.

the plus mode and (b) is for the minus mode, and $\Gamma=(0,0)$, $X=(0,\pi)$, $M=(\pi,\pi)$ in momentum space.

It is obvious from Fig. 8 that $S_+(\boldsymbol{k})$ of the ordered state ($\alpha=0.4$, 2.4) is proportional to k near the Γ point and $S_-(\boldsymbol{k})$ has an antiferromagnetic peak at the M point. On the other hand, $S_+(\boldsymbol{k})$ at $\alpha=3.6$ increases quadratically with k near the Γ point [see the inset of Fig. 8(a)]. In the Néel state, the excitation is gapless at two points. One is $\omega_+(\boldsymbol{k})$ at the Γ point. Around this point, since the function $f_+(\boldsymbol{k})$ in Eq. (35) behaves as $f_+(\boldsymbol{k})\propto k^2$ and the structure factor as $S_+(\boldsymbol{k})\propto k$, the excitation is proportional to k. The other is $\omega_-(\boldsymbol{k})$ at the M point where $S_-(\boldsymbol{k})$ diverges due to the antiferromagnetic long-range order. Thus the gap opens when the structure factor becomes proportional to the square of k for the former point and when the structure factor does not diverge, that is, the system becomes the disordered state for the latter point. In the former case, we should determine the critical coupling α_{c2} where the gap opens. We take five k_x points and do the following fitting along the Γ-X line: $S_+(k_x)=a_1k_x+a_2k_x^2+a_3k_x^3$, where a_1,a_2, and a_3 are fitting parameters. The result of a_1 versus α is shown in Fig. 7 (open squares). Comparing the result of staggered magnetization with this coefficient, we find that the critical point α_{c2} is equal to α_c within the statistical and fitting errors, which gives $\alpha_c=3.51\pm0.05$. The α dependence of the gap is shown in Fig. 10. All values are scaled by $J_\parallel$. Open circles are for $\omega_+(0,0)$ and closed circles are for $\omega_-(\pi,\pi)$. In the disordered phase, the excitation energy $\omega_-(\pi,\pi)$ always takes a smaller value. The spin wave velocity along the Γ-X line is calculated for the ordered state and the result is shown in the inset of Fig. 10. Here, Z_c is the renormalization factor; namely, the spin wave velocity is given by $\sqrt{2}Z_cJ_\parallel$. As the coupling increases, the velocity first slightly decreases and then suddenly increases near the critical point.

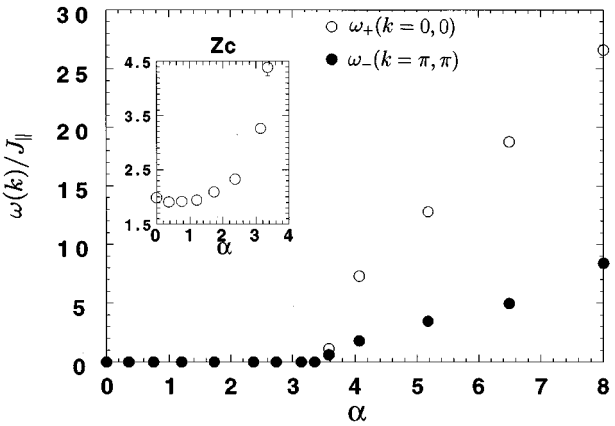

FIG. 10. The α dependence of the gap for $\omega_+(0,0)$ and $\omega_-(\pi,\pi)$. In the inset, the renormalization factor of the linear spin wave velocity, Z_c, is also shown.

VI. DISCUSSION

In this paper we first solved the Hamiltonian by the Schwinger-boson mean-field theory. Then the solution was Gutzwiller projected to obtain variational ground-state wave functions, which were examined by Monte Carlo simulation for finite sizes.

We first see the advantage of our variational Monte Carlo simulation. In the mean-field calculation, the system becomes dimerized for $\alpha > 4.62$. For this region, the interlayer order parameter $\Delta_\parallel$ is zero and only dimer coupling between the layers is permitted. In addition, the excitation spectrum becomes flat in momentum space: $E_g(k) = \sqrt{\lambda^2 - \delta^2}$. As a matter of fact, theoretically, this state must only be realized at $\alpha \to \infty$. This disadvantage is removed in Monte Carlo simulation. It is estimated from Fig. 4 that the virtual critical point where the system stabilizes with the dimerized state is 11.0. This means that the Gutzwiller projection improves the wave functions. The improved wave function can describe the disordered state without dimerization at least up to $\alpha = 11.0$.

There have been many investigations for the order-disorder critical point. Our mean-field result is essentially the same as those of the previous report[7] and the modified spin wave theory.[13] These give the critical value of α around 4.5.[31] This value is much larger than the results by other methods: 2.56 by the dimer expansion, and 2.51 ± 0.01 by the quantum Monte Carlo method. However, these latter values are still formidably larger than the value of α realized in the bilayer cuprates. Our motivation for this work was to see if our method gives a critical value closer to the experimental value or not. Our result, $\alpha_c = 3.51 \pm 0.05$,[32] does not meet this expectation, and confirms the previous theories that without doping the bilayer Heisenberg model will not give an explanation for the spin gap behavior of the experiments.

We also calculated the excitation spectrum, especially for the disordered phase. It is not obvious whether the system has always a finite gap in the disordered state. For instance, there is no long-range order for the one-dimensional $s = 1/2$ antiferromagnetic Heisenberg model, though the excitation spectrum is gapless. In our bilayer two-dimensional Heisenberg model, we find that there is always a finite gap for the disordered state. Within the statistical and fitting errors, it occurs at $\alpha_c = 3.51 \pm 0.05$. In the disordered region, the spin-spin correlation decays exponentially with distance. The structure factor $S_-(\boldsymbol{k})$ near the critical coupling, however, has a large maximal value at the M point, which minimizes the excitation spectrum at that point. This shows that even in the disordered state the antiferromagnetic spin fluctuation is strong. It should be remarked that even though the spectrum $\omega_-(\boldsymbol{k})$ at $\alpha = 3.6$ looks singular at $\boldsymbol{Q} = (\pi, \pi)$, this is not the case. Around $\boldsymbol{Q}$ it should be quadratic in $(\boldsymbol{k} - \boldsymbol{Q})$. Such a behavior is not apparent in Fig. 9(b) due to the lack of data close enough to $\boldsymbol{Q}$.

At $\alpha = 0$ where the model becomes the single-layer Heisenberg model, our result can be compared with other methods: spin wave theory, series expansions, and the single-mode approximation.[33–35] Our result for the spectrum is roughly proportional to those of other methods over the entire Brillouin zone. The maximal value is around $2.65 J_\parallel$ at X or $L = (\pi/2, \pi/2)$. Series expansions predict the maximum is about $2.35 J_\parallel$ at the L point[34] and the single-mode approximation based on the expansions around the Ising limit estimates the maximum about $2.5 J_\parallel$ at L point.[35] Both results are close to our result. The most remarkable difference from the other methods is the spin wave velocity. The renormalization factor Z_c is 1.99 ± 0.03 at $\alpha = 0$ which is 1.69 times larger than the best estimated value, around 1.18 ± 0.02.[36] This difference indicates that multimagnon contribution to $S_+(\boldsymbol{k})$ is not negligible. However, since this method gives a qualitatively correct behavior, we believe it gives qualitatively correct spectrum at $\alpha > 0$ also. Finally, we remark that the non-monotonic behavior of the spin wave velocity with increasing interlayer coupling can be understood from that of the coefficient (a_1) of the structure factor shown in Fig. 7, since the spin wave velocity is inversely proportional to a_1.

In conclusion, we have investigated the bilayer Heisenberg model using the Schwinger-boson Gutzwiller-projection method. We find that there is an order-disorder transition with increasing interlayer coupling. The critical point is $\alpha_c = 3.51 \pm 0.05$. The excitation spectrum can be calculated for a wide range of coupling and we find that the spin excitation always has a finite gap for the disordered phase and the minimum of the spectrum is located at the M point. Our model corresponds to the half-filled case for high-T_c cuprates. Although α_c in this case is quite large, it is possible that hole doping reduces the value extremely. Then it will be possible that our disordered state continuously changes into the spin gap state. A similar treatment for a hole doped model, the t-t'-J model, is our next problem.

ACKNOWLEDGMENTS

The authors thank M. Ogata for useful comments on the results of our Monte Carlo simulations.

[1] M. Takigawa, A. P. Reyes, P. C. Hammel, J. D. Thompson, R. H. Heffner, Z. Fisk, and K. C. Ott, Phys. Rev. B **42**, 243 (1991).
[2] J. M. Tranquada, P. M. Gehring, G. Shirane, S. Shamoto, and M. Sato, Phys. Rev. B **46**, 5561 (1992).
[3] K. Yamada, Y. Endoh, C. H. Lee, S. Wakimoto, M. Arai, K. Ubukata, M. Fujita, S. Hosoya, and S. M. Bennington, J. Phys. Soc. Jpn. **64**, 2742 (1995).
[4] B. L. Altshuler and L. B. Ioffe, Solid State Commun. **82**, 253 (1992).
[5] B. L. Altshuler, L. B. Ioffe, A. I. Larkin, and A. J. Millis, JETP Lett. **59**, 65 (1994).
[6] M. Ubbens and P. A. Lee, Phys. Rev. B **50**, 438 (1994).
[7] A. J. Millis and H. Monien, Phys. Rev. Lett. **70**, 2810 (1993).
[8] A. J. Millis and H. Monien, Phys. Rev. B **50**, 16 606 (1994).
[9] A. Sokol and D. Pines, Phys. Rev. Lett. **71**, 2813 (1993).
[10] A. W. Sandvik, A. V. Chubukov, and S. Sachdev, Phys. Rev. B **51**, 16 483 (1995).
[11] A. V. Chubukov and D. K. Morr, Phys. Rev. B **52**, 3521 (1995).

[12] T. Matsuda and K. Hida, J. Phys. Soc. Jpn. **59**, 2223 (1990).
[13] K. Hida, J. Phys. Soc. Jpn. **59**, 2230 (1990).
[14] A. W. Sandvik and D. J. Scalapino, Phys. Rev. Lett. **72**, 2777 (1994).
[15] K. Hida, J. Phys. Soc. Jpn. **61**, 1013 (1992).
[16] D. P. Arovas and A. Auerbach, Phys. Rev. Lett. **61**, 316 (1988).
[17] A. Auerbach and D. P. Arovas, Phys. Rev. B **38**, 617 (1988).
[18] P. W. Anderson, Mater. Res. Bull. **8**, 153 (1973).
[19] P. W. Anderson, Science **235**, 1196 (1987).
[20] S. Liang, B. Douçot, and P. W. Anderson, Phys. Rev. Lett. **61**, 365 (1988).
[21] Y. C. Chen and K. Xiu, Phys. Lett. A **181**, 373 (1993).
[22] T. Miyazaki, D. Yoshioka, and M. Ogata, Phys. Rev. B **51**, 2966 (1995).
[23] H. A. Bethe, Z. Phys. **71**, 205 (1931).
[24] D. Yoshioka, J. Phys. Soc. Jpn. **58**, 32 (1989).
[25] D. Yoshioka, J. Phys. Soc. Jpn. **58**, 3733 (1989).
[26] R. P. Feynman, Phys. Rev. **94**, 262 (1954).
[27] R. P. Feynman and M. Cohen, Phys. Rev. **102**, 1189 (1956).
[28] R. R. P. Singh and D. A. Huse, Phys. Rev. B **40**, 7247 (1989).
[29] N. Trivedi and D. M. Ceperley, Phys. Rev. B **40**, 2737 (1989).
[30] D. A. Huse, Phys. Rev. B **37**, 2380 (1988).
[31] Schwinger-boson mean-field theory and the modified spin wave theory are essentially the same. In the present system, the latter has given a smaller critical value because the possibility of the first-order phase transition is considered.
[32] In terms of α_p this transition occurs at $\alpha_p = 2.57 \pm 0.02$.
[33] J. Igarashi and A. Watabe, Phys. Rev. B **43**, 13 456 (1991); **44**, 5057 (1991).
[34] R. R. P. Singh and M. P. Gelfand (unpublished).
[35] R. R. P. Singh, Phys. Rev. B **47**, 12 337 (1993).
[36] E. Manousakis, Rev. Mod. Phys. **63**, 1 (1991).